Journal of Engineering Mathematics **33:** 219–236, 1998.

The steady-state microwave heating of slabs with small Arrhenius absorptivity

T. R. MARCHANT and B. LIU
Department of Mathematics, The University of Wollongong, Northfields Ave., Wollongong, N.S.W., 2522, Australia,
e-mail: tim_marchant@now.edu.au

Received 30 August 1996; accepted in revised form 17 June 1997

Abstract. The steady-state microwave heating of a finite one-dimensional slab is examined. The temperature dependency of the electrical conductivity and the thermal absorptivity is assumed to be governed by the Arrhenius law, while both the electrical permittivity and magnetic permeability are assumed constant. The governing equations are the steady-state versions of the forced heat equation and Maxwell's Equations while the boundary conditions take into account both convective and radiative heat loss. Approximate analytical solutions, valid for small thermal absorptivity, are found for the steady-state temperature and the electric-field amplitude using the Galerkin method. As the Arrhenius law is not amenable analytically, it is approximated by a rational-cubic function. At the steady-state the temperature versus power relationship is found to be multivalued; at the critical power level thermal runaway occurs when the temperature jumps from the lower (cool) temperature branch to the upper (hot) temperature branch of the solution. The approximate analytical solutions are compared with the numerical solutions of the governing equations in the limits of small and large heat-loss and also for an intermediate case involving radiative heat-loss.

Key words: microwave heating, thermal runaway, Arrhenius law, steady-state, small thermal absorptivity

1. Introduction

There is growing interest in the use of microwave radiation in industrial processes such as drying, smelting, sintering, melting and sterilising. The main advantage of microwave heating over conventional convective heating methods is that the processing time can be dramatically reduced. The microwave processing of a material can be difficult to control however; thermal runaway can occur for a small increase in the incident power, resulting in a large and rapid increase in the material's temperature.

The equations governing the microwave heating of a material are Maxwell's Equations governing the propagation of microwave radiation through the material, and the forced heat equation governing the heat absorption and the resultant heat diffusion, with the heat absorption being proportional to the square of the amplitude of the electric field. In general, the properties of the material, such as electrical conductivity, electrical permittivity and magnetic permeability are temperature dependent. As the rate of heat absorption in the material increases with temperature, hence as the temperature increases so does the heat absorption, which can then lead to thermal runaway. Thermal runaway, can sometimes be beneficial to the industrial process, such as in the smelting of metals, but is usually harmful, such as in the drying of wool (see Araneta *et al*. [1]) or in the sintering of ceramics.

Due to its destructive nature, it is important to understand and hence predict the occurence of thermal runaway. The governing equations of microwave heating are coupled in a nonlinear manner through the temperature dependence of the material properties and consequently

exact analytical solutions are rarely available. Also, numerical solutions are computationally expensive, particularly for a realistic three-dimensional geometry appropriate for an industrial process. Due to the difficulties with both exact and numerical solutions, the aim of this paper is to develop an approximate analytical solution which can describe and predict thermal runaway.

The mathematical modelling of microwave heating has generated a lot of interest in the last few years; the survey article of Hill and Marchant [2] details much of this work. If the initial propagation of microwave radiation, and the subsequent heating of the material are of interest, then perturbation solutions for the electric field and the temperature can be found. Smyth [3] and Marchant and Pincombe [4] considered high-frequency radiation (the geometrical optics limit) and small thermal diffusivity to develop perturbation solutions using the method of strained co-ordinates with the electrical conductivity, electrical permittivity and magnetic permeability all assumed to be slowly-varying with a power-law dependence on temperature. Smyth [3] found series solutions for a semi-infinite slab, cylindrically symmetric and spherically symmetric bodies, while Marchant and Pincombe [4] developed perturbation solutions which illustrate the process of thermal runaway and compared it to numerical solutions of the governing equations.

Pincombe and Smyth [5] considered all the material properties to be slowly-varying functions of space and time. In addition, the electrical conductivity and thermal absorptivity were assumed to be small. A perturbation solution was developed using the method of multiple scales and in the case of constant microwave speed some analytical solutions for the first-order amplitude were found, including cases where thermal runaway occurs. In addition, numerical solutions were developed for the case in which the wavespeed is temperature dependent.

Alternatively, if the thermal aspects are isolated, the forced heat equation

$$T_t = \nu T_{xx} + \gamma(T), \tag{1.1}$$

is considered, where $\gamma(T)$ is the temperature dependent rate of microwave absorption by the material (the thermal absorptivity) and the constant electric-field amplitude is normalised to unity. Roussy et al. [6] numerically solved (1.1) for a cylindrical body with the thermal absorptivity dependent on a quadratic function of temperature

$$\gamma = \gamma_0 + \gamma_1 T + \gamma_2 T^2, \tag{1.2}$$

with a convective heat-loss boundary condition. Hill and Smyth [7] considered (1.1) for planar, cylindrical and spherical geometries with a fixed temperature boundary condition and found steady-state solutions. They assumed that in the regions of parameter space where steady-state solutions do not occur, thermal runaway does, due to the exponential thermal absorptivity. Also, for some parameter values, two steady-state solutions exist, with the higher temperature profile unstable and the lower temperature profile stable.

Marchant [9] in a study of materials with impurities and microwave joining considered

$$\gamma = \gamma_0 + (\gamma_1 + \gamma_2 T^{\gamma_3})\delta(x), \tag{1.3}$$

where $\delta(x)$ is the Dirac-delta function. This represented a material of constant thermal absorptivity with an impurity at $x = 0$. At the impurity there is a source of additional temperature-dependent thermal absorptivity. Steady-state solutions and conditions for thermal runaway were found for a one-dimensional slab.

Zhu *et al.* [9] considered various versions of the one and two-dimensional forced heat equations as models for microwave joining and welding. For these models exact steady-state solutions did not exist, however approximate governing equations were found using a method developed by Frank–Kamenetskii in the study of chemical reactions. This allowed approximate conditions for thermal runaway to be developed, which were found to be very close to the numerical results.

Kriegsmann *et al.* [10] considered a semi-infinite material with temperature-dependent electrical conductivity and constant magnetic permeability and electrical permittivity. The electrical conductivity was assumed to be small and a perturbation solution was found as a series in the low conductivity. Because a radiative boundary condition was used, heat can escape from the material and hence steady-state solutions occur. For this model there is one steady-state temperature profile for each power level so thermal runaway does not occur.

Kriegsmann [11] derived a steady-state solution for a finite one-dimensional slab by expanding the temperature and electric-field amplitude as a perturbation series in the small Biot-number. As there was small heat-loss through the boundaries the temperature profile was found to be uniform in this limit. This allowed the forced heat equation to be integrated over the slab which gave an equation describing the relationship between the steady-state power and temperature. The temperature versus power curve was an S-shaped curve implying thermal runaway occurs at a critical power level as the solution jumps to a stable high temperature solution. As the electric-field amplitude and the temperature are coupled, the thermal runaway is stabilised at a new hot steady-state because the increased temperature causes decay of the electric-field amplitude in the slab which in turn limits the heat absorption. The results obtained contained those of the thin slab and thick slab as limiting cases.

In a related study Kriegsmann [12] derived a nonlinear amplitude equation which described the time evolution of the material's temperature in the small Biot-number limit. Depending on the initial conditions, such as the incident microwave power, the system either evolved to the lower (cool) branch of the S-shaped curve mentioned above or to the upper (hot) branch.

Marchant and Kriegsmann [13] considered the forced heat equation and a steady-state version of Maxwell's Equations together with boundary conditions appropriate for one-dimensional slab. The Rayleigh–Ritz method was used to develop approximate analytical expressions for the temperature and electric-field amplitude together with an ordinary differential equation describing the evolution of the temperature to the steady-state . At the steady-state the temperature versus power relationship is S-shaped. Power-law and exponential temperature dependencies were considered for the electric conductivity (which is assumed small) and thermal absorptivity. Examples were presented in both the small and large Biot-number limits with a good comparison obtained between the approximate analytical solutions and the numerical solutions.

In this paper the steady-state heating of a one-dimensional slab by microwave radiation is considered with the temperature dependencies of the electrical conductivity and thermal absorptivity governed by the Arrhenius law. Both the electrical permittivity and the magnetic permeability are assumed constant. In Section 2 the governing equations are derived. These are steady-state versions of the forced heat equation, which describes the absorption and diffusion of heat and Maxwell's Equations which describes the electric-field amplitude in the slab. In Section 3 the method of Marchant and Kriegsmann [13] is used to develop approximate expressions, valid for small thermal absorptivity, for the steady-state temperature and electric-field amplitude in the slab. In order to develop these approximate analytical solutions the Arrhenius law is approximated by a rational-cubic function. Examples are presented in the

limits of small and large heat-loss and for an intermediate case, which involves radiative heat-loss. The approximate analytical solutions of Section 3 are compared with numerical solutions of the governing equations. In Section 4 some concluding remarks are made and future extensions, to models of microwave heating in higher-dimensions, discussed. The scheme used for the numerical solutions is detailed in the appendix.

2. Governing equations

The equations which govern the microwave heating of a material are Maxwell's Equations, which govern the propagation of the microwave radiation, and the forced heat equation, which governs the absorption and diffusion of heat by the material. Maxwell's Equations of electormagnetism are (see Portis [14], p. 381–384)

$$\begin{aligned} &\nabla \cdot (\varepsilon \mathbf{E}) = \rho, \quad \nabla \cdot (\mu \mathbf{H}) = 0, \\ &\nabla \times \mathbf{E} = -\frac{\partial}{\partial t}(\mu \mathbf{H}), \quad \nabla \times \mathbf{H} = \frac{\partial}{\partial t}(\varepsilon \mathbf{E}) + \sigma \mathbf{E}, \end{aligned} \tag{2.1}$$

where $\mathbf{E}$ is the electric field, and $\mathbf{H}$ is the magnetic field. The material properties are σ, the electrical conductivity, ε, the electrical permittivity and μ, the magnetic permeability. The electrical conductivity is dependent on the temperature whilst the magnetic permeability and electrical permittivity are assumed constant.

For a plane wave propagation in a slab we have $\mathbf{E} = E(x,t)\mathbf{j}$ and $\mathbf{H} = H(x,t)\mathbf{k}$, which when substituted into (2.1) gives

$$E_x = -\mu H_t, \quad H_x = -\varepsilon E_t - \sigma E, \tag{2.2}$$

where it has been assumed that the net free charge ρ is zero. The electric and magnetic fields are written as amplitude terms modulated by the frequency

$$E(x,t) = U(x)\,\mathrm{e}^{-i\omega t}, \quad H(x,t) = V(x)\,\mathrm{e}^{-i\omega t}. \tag{2.3}$$

As the time scale for electromagnetic propagation is much smaller than the time scale for thermal diffusion the time derivatives of the electric and magnetic field amplitudes, U and V, and of the electrical conductivity, σ, can be ignored. Substituting (2.3) in (2.2) gives

$$U_{xx} + k_1^2 \left(1 + \frac{i\sigma}{\omega\varepsilon}\right) U = 0, \tag{2.4}$$

as the governing equation for the steady-state electric-field amplitude, where the wavenumber $k_1 = \omega/c$, with c being the speed of the radiation in the material. Note that the same governing Equation (2.4) is obtained even when the electrical permittivity depends on temperature; the later analysis is simplified however, by the assumption of constant electrical permittivity.

Equation (2.4) is coupled with the forced heat equation

$$T_t = \nu T_{xx} + \gamma(T)|U|^2,$$

where

$$\sigma = \alpha f(T), \quad \gamma = \beta f(T), \tag{2.5}$$

where ν is the thermal diffusivity which is assumed constant and γ is the thermal absorptivity which is temperature dependent. The thermal absorption depends on the square of the electric-field amplitude. The time harmonic form of electric field (2.3) means that the heat source term has been averaged over a microwave period (see Kriegsmann *et al.* [10]). The same form of temperature dependency $f(T)$, is chosen for the electrical conductivity and the thermal absorptivity as physically it is expected from conservation of energy that the energy lost by the microwaves is absorbed as heat.

The electric field and its derivative are continuous at the boundaries of the slab $(x = \pm l)$ so the boundary conditions are

$$\begin{aligned} &E_x(-l,t) + ikE(-l,t) = 2ikE\,\mathrm{e}^{-i\omega t}, \\ &E_x(l,t) - ikE(l,t) = 0, \end{aligned} \tag{2.6}$$

where $k = \omega/c_0$. The parameters k and c_0 are the wavenumber and velocity of the radiation in free space respectively.

The steady-state amplitude Equation (2.4), the steady-state version of the forced heat equation (2.5) and the boundary conditions for the electric field (2.6) are made non-dimensional by the scalings

$$t' = \frac{t\nu}{l^2}, \quad x' = \frac{x}{l}, \quad E' = \frac{E}{E_i}, \quad T' = \frac{T}{T_i} - 1, \tag{2.7}$$

where $2l$ is the length of the slab, E_i is the amplitude of the incident radiation, ν is the thermal diffusivity and T_i is the ambient temperature. This results in the scaled frequency, thermal absorptivity, electrical conductivity and wavenumbers having the forms

$$\omega' = \frac{\omega l^2}{\nu}, \quad \gamma' = \frac{l^2 E_i^2 \gamma}{\nu T_i}, \quad \sigma' = \frac{\sigma}{\omega\varepsilon}, \quad k_1' = k_1 l, \quad k' = kl. \tag{2.8}$$

The steady-state governing equations can then be written (after dropping the primes) as

$$U_{xx} + k_1^2(1 + i\sigma)U = 0, \quad T_{xx} + \gamma|U|^2 = 0, \tag{2.9}$$

where the Arrhenius law,

$$f(T) = \alpha_1 + \beta_1\,\mathrm{e}^{-(\gamma_1/T)}, \tag{2.10}$$

is used for the temperature dependency. This law is physically motivated from statistical mechanics and is bounded as the temperature becomes large.

The boundary conditions for the electric field amplitude and the temperature are

$$\begin{aligned} &U_x + ikU = 2ik, \quad x = -1, \quad U_x - ikU = 0, \quad x = 1, \\ &T_x \pm B_i T \pm S((T+1)^4 - 1) = 0, \quad x = \pm 1, \end{aligned} \tag{2.11}$$

where both convective and radiative heat loss occurs at each end of the slab. The Biot number, B_i, is a measure of the convective heat loss and the radiation-number S, is a measure of the radiative heat loss. Note that the ambient temperature has been scaled to zero. In the small heat loss limit $(B_i, S \to 0)$ a zero heat flux boundary condition is obtained. In the large heat-loss

limit ($B_i, S \to \infty$) a fixed temperature boundary condition is applied. The thermally insulated boundary condition is a good approximation for dielectric materials as the Biot and radiation numbers are small (for example, $B_i, S \sim 10^{-4}$ for ceramics, see Kriegsmann [13]).

Usually the material properties are measured experimentally in terms of the relative dielectric constant ε' and the relative dielectric loss ε''. In terms of the non-dimensional parameters of (2.8) they can be written as

$$\varepsilon' = \frac{k_1^2}{k^2}, \quad \varepsilon'' = \frac{k_1^2 \sigma}{k^2}. \tag{2.12}$$

In a semi-infinite material with small electrical conductivity the electric-field amplitude in the slab is given by

$$U(x) = U_0 \, \mathrm{e}^{-k_1 \sigma (x/2)}. \tag{2.13}$$

Hence the electric-field amplitude decays on a length scale of $(k_1\sigma)^{-1}$. Due to the scaling of k_1 (see (2.8)), the decay length scale increases as the slab length $l \to 0$. Hence the thin-slab limit with constant electric-field amplitude is obtained. Conversely, the thick-slab limit $l \to \infty$ results in the decay length scale decreasing to zero. Here a 'skin effect' results with the electric-field amplitude decaying quickly to zero in the slab. It should be noted that the frequency of the microwave radiation affects the decay of the electric-field amplitude also (see the scaling of σ in (2.8)). For example, increasing the frequency, ω, decreases the scaled electrical conductivity, resulting in a longer decay length. By calculating the decay length scale $(k_1\sigma)^{-1}$ from the associated parameters it is possible to determine if either the thick or thin-slab limit is appropriate for a particular example.

3. Approximate steady-state solutions

In this section approximate analytical expressions for the steady-state temperature and the electric-field amplitude in the slab are developed. At the steady state the temperature versus power relationship is found, which is described by a S-shaped curve, hence thermal runaway occurs at a critical power level as the solution jumps from the lower (cool) branch to the upper (hot) branch of the solution.

3.1. The rational-cubic approximation

The Arrhenius law (2.10) is a physically appropriate choice of temperature dependency for the electrical conductivity and the thermal absorptivity. However, it is unsuitable for analytical work, so an approximation to (2.10) must be used. Marchant [15] showed that a rational-cubic function was an extremely accurate approximation to the Arrhenius law in the case of the microwave welding of a one-dimensional slab. Hence a rational-cubic function of the form

$$f(T) = \frac{R_1(T)}{R_2(T)},$$

where

$$\begin{aligned} &R_i(T) = \sum_{j=0}^{3} r_{ij} T^j, \quad i = 1, 2, \\ &r_{10} = \alpha_1, \quad r_{20} = 1, \quad r_{13} = (\alpha_1 + \beta_1) r_{23}, \end{aligned} \tag{3.1}$$

is used to approximate the Arrhenius law here. At the ambient temperature, the rational-cubic function $f(0) = \alpha_1$, while $f \to \alpha_1 + \beta_1$ as $T \to \infty$. Hence the rational-cubic function is the same as the Arrhenius law (2.10) in the limits of small and large temperatures. The remaining parameters (the undetermined $r_{i,j}$) are chosen using the method of least squares. The sum of the squares

$$S = \sum_{i=1}^{n} \left(\alpha_1 + \beta_1 \, \mathrm{e}^{-(\gamma_1/T_i)} - \frac{R_1(T_i)}{R_2(T_i)} \right)^2, \quad T_i = \frac{i}{n} T_0, \tag{3.2}$$

over the temperature range $T \in [0, T_0]$ is considered. The sum S is minimised if the r_{ij} are chosen to satisfy

$$\frac{\partial S}{\partial r_{ij}} = 0. \tag{3.3}$$

Note that (3.3) represents five nonlinear algebraic equations for the undetermined parameters. In the subsequent sections the Arrhenius law (2.10) is considered with the parameters

$$\alpha_1 = \gamma_1 = 1, \quad \beta_1 = 20. \tag{3.4}$$

The Equations (3.3) are solved using the IMSL routine, dnegnf, which gives the parameters as

$$\begin{aligned} &r_{11} = 5{\cdot}469, \quad r_{12} = -43{\cdot}34, \quad r_{21} = 2{\cdot}534, \\ &r_{22} = 8{\cdot}255, \quad r_{23} = 10{\cdot}71. \end{aligned} \tag{3.5}$$

The parameters (3.5) were found with $T_0 = 10$ and $n = 2 \times 10^7$ in (3.2). The average deviation between the Arrhenius law (2.10) and the rational-cubic function (3.1) at each point in the sum is $\sqrt{\frac{S}{n}} = 0{\cdot}013$. The error in the approximation is largest at low temperature levels (up to 4 percent near $f = 1$), while at higher temperature levels the error is insignificant.

Besides the Arrhenius law, other forms of temperature dependency are valid for some materials. Hill and Jennings [8] analysed the experimental data collected for various materials and found various simple analytical forms for $f(T)$. They found that, in general, the thermal absorptivity increases with temperature. However, it can also decrease with temperature over a limited temperature range. In particular, they found linear, quadratic and exponential dependencies, of the form $\alpha \, \mathrm{e}^{\beta T}$ and $\alpha \, \mathrm{e}^{-\beta(Y-\gamma)^2}$, are valid for many materials. Like the Arrhenius law, the exponential dependencies are not amenable to analysis and would need to be approximated by a polynomial function. Hill and Jennings [16] showed to get a good fit to the various exponential dependencies that a quintic function needs to be used. The approximate method developed in this section would be able to deal with quintic functions quite easily; the resulting expressions will just be longer and more complicated. The rational-cubic approximation for the Arrhenius law is valid for all temperatures, while a polynomial approximation to an exponential dependency can only be valid over a finite temperature range. However, as long as the polynomial approximation is valid for the temperature range over which thermal runaway occurs, the approximate analytical solutions can be expected to be accurate.

3.2. THE APPROXIMATE EQUATIONS

In the small heat-loss limit Kriegsmann [11] found that the temperature profile in the slab to lowest-order was uniform which allows the steady-state amplitude equation (the first of (2.9)) to be solved exactly and the steady-state temperature versus power relationship to be found by integrating the forced heat equation over the slab. Here this method is generalised for arbitrary Biot and radiation numbers by assuming basis functions, which satisfy the boundary conditions (2.11), for the temperature and the electric-field amplitude. The parameters associated with the trial solutions are found by applying the Galerkin method, which requires the basis functions to satisfy averaged versions of the governing Equations (2.9). The resulting expressions then describe the temperature and electric-field amplitude at the steady state. In addition the steady-state temperature versus power relationship is obtained.

Firstly, the governing Equations (2.9) are written in the form

$$\begin{aligned} &T_{xx}R_2(T) + \beta R_1(T)|U|^2 = 0, \\ &U_{xx}R_2(T) + k_1^2(R_2(T) + i\alpha R_1(T))U = 0, \end{aligned} \tag{3.6}$$

where the Arrhenius law (2.10) has been approximated by the rational-cubic function (3.1). In addition both equations have been multiplied by the denominator of the rational-cubic function so that analytically amenable expressions are obtained.

Generally, the Galerkin method requires that the exact solution be approximated by a sum of orthogonal basis functions. The parameters associated with the basis functions are found by evaluating averaged versions of the governing equations, weighted by the basis functions themselves. Here the simplest application of the method is used, with both the electric-field amplitude and the temperature each represented by one basis function only. The approximate solutions have the form

$$T(x) = C\phi_1(x), \quad U(x) = \phi_2(x, a), \tag{3.7}$$

where C and a are parameters to be determined. The basis functions (3.7) for the temperature and the electric-field amplitude will be chosen to satisfy the boundary conditions (2.11) exactly, but will satisfy averaged versions of the governing equations

$$\begin{aligned} &\int_{-1}^{1} \omega_1(C\phi_{1xx}R_2(C\phi_1) + \beta R_1(C\phi_1)|\phi_2|^2)\,\mathrm{d}x = 0, \\ &\int_{-1}^{1} \omega_2(\phi_{2xx}R_2(C\phi_1) + k_1^2(R_2(C\phi_1) + i\alpha R_1(C\phi_1))\phi_2)\,\mathrm{d}x = 0, \end{aligned} \tag{3.8}$$

where the integrals are weighted by ω_1 and ω_2, normally chosen as the basis functions ϕ_1 and ϕ_2 respectively.

To find a suitable basis function for the temperature the time-dependent unforced heat Equation ((2.3) with $\gamma = 0$ and $\nu = 1$) subject to a convective heat-loss boundary condition ((2.11) with $S = 0$) is considered. This has the solution

$$T(x,t) = \sum_{n=1}^{\infty} a_n\,\mathrm{e}^{-\lambda_n t}\cos(\lambda_n^{1/2}x), \quad B_i = \lambda_n^{1/2}\tan(\lambda_n^{1/2}), \tag{3.9}$$

where the coefficients a_n are determined from the initial temperature profile. The solution describes the decay from the initial profile to the ambient temperature as heat is convected away through the boundaries. Hence

$$\phi_1(x) = \cos(\lambda^{1/2}x), \tag{3.10}$$

is chosen as the basis function for the temperature. The temperature profile (3.7) is symmetric with a maximum C at the slab's centre. This approximate solution will be valid when the thermal absorption of microwave energy is fairly small, which generally means the lower (cooler) branch of the S-shaped power versus temperature curve.

When no radiative heat-loss occurs λ in (3.10) corresponds to the smallest eigenvalue of (3.9). The basis function is then valid at long time as it decays more slowly than the other eigenfunctions. If the radiative heat-loss is finite then the value of λ changes. The boundary condition (2.11) gives the transcendental equation

$$B_i = \lambda_1 \tan\lambda_1 - S(C^3\cos^3\lambda_1 + 4C^2\cos^2\lambda_1 + 6C\cos\lambda_1 + 4), \tag{3.11}$$

for λ, where $\lambda_1 = \lambda^{1/2}$. The heat-loss parameter λ is a measure of the combined convective and radiative heat-loss. The parameter λ varies from zero, in the limit of no heat-loss, to $\pi^2/4$, in the large heat-loss limit. When no radiative heat-loss occurs the heat-loss parameter λ is fixed. But when the radiation-number is finite λ varies as the temperature C changes.

The basis function for the electric-field amplitude is chosen as

$$\begin{aligned} &\phi_2(x) = A(a)\cosh(ax) + B(a)\sinh(ax),\\ &A(a) = -ik(a\sinh(a) - ik\cosh(a))^{-1},\\ &B(a) = ik(a\cosh(a) - ik\sinh(a))^{-1}, \end{aligned} \tag{3.12}$$

where the constants A and B are found from the boundary condition (2.11). This form of basis function is chosen as it is the solution of the first of (2.9) in the special case of constant electrical conductivity, in which case the decay rate is

$$a = ik_1(1 + i\sigma)^{1/2}. \tag{3.13}$$

For the general case when the electrical conductivity is temperature dependent, the decay rate a is found from the averaged amplitude equation (the second of (3.8)), using the weight $\omega_2 = \phi_2^{-1}$. This gives the decay rate as

$$a(C) = ik_1\left[1 + i\alpha\left(\frac{\int_{-1}^{1} R_1(C\phi_1)\,\mathrm{d}x}{\int_{-1}^{1} R_2(C\phi_1)\,\mathrm{d}x}\right)\right]^{1/2}. \tag{3.14}$$

This choice of weight, $\omega_2 = \phi_2^{-1}$, is unusual, however it is chosen as it gives a simple explicit expression for the decay rate a. The more usual weight $\omega_2 = \phi_2$, gives an implicit relationship for a which, together with (3.16), would need to be solved numerically for a and C. Moreover, numerical calculations show that there is very little change in the decay rate a in the large heat-loss limit when the choice of weight is varied (the choice of weight makes no difference to a in the small heat-loss limit).

Substituting for the basis function (3.10) in (3.14) gives

$$a(C) = ik_1 \left(1 + i\alpha \frac{I_1}{I_2}\right)^{1/2},$$

where

$$\begin{aligned} I_i \;=\; & 2r_{i0} + 2r_{i1} C \frac{\sin(\lambda_1)}{\lambda_1} + r_{i2} C^2 \left(1 + \frac{\sin(2\lambda_1)}{2\lambda_1}\right) \\ & + r_{i3} C^3 \left(\frac{3\sin(\lambda_1)}{2\lambda_1} + \frac{\sin(3\lambda_1)}{6\lambda_1}\right), \quad i = 1, 2, \end{aligned} \tag{3.15}$$

for the decay rate a. Using the weight $\omega_1 = \phi_1$ in the averaged forced heat equation (the first of (3.8)) leads to the following transcendental equation

$$\beta = \frac{\lambda C g_2}{g_1},$$

where

$$\begin{aligned} g_1(C, a) \;&=\; \int_{-1}^{1} \phi_1 R_1(C\phi_1) |\phi_2|^2 \, \mathrm{d}x, \\ g_2(C, a) \;&=\; \int_{-1}^{1} \phi_1^2 R_2(C\phi_1) \, \mathrm{d}x. \end{aligned} \tag{3.16}$$

The parameter β is the ratio of the steady-state power absorbed by the material to the heat lost at the boundaries due to convection and radiation. Since γ has been scaled by the square of the incident electric-field amplitude, E_i^2, (see (2.8)) the parameter β is proportional to the incident power. Hence the expression (3.16) gives the dimensionless power as a function of the temperature C. The expression (3.16) is simply referred to as the temperature versus power (C versus β) curve.

In order to facilitate the calculation of the integral g_1 in (3.16) the square of the electric-field amplitude is written as

$$|\phi_2|^2 = a_1 \cosh(2ux) + b_1 \cos(2vx),$$

where

$$a = u + iv, \quad 2a = A\bar{A} + B\bar{B}, \quad 2b_1 = A\bar{A} - B\bar{B}. \tag{3.17}$$

The new parameters a_1, b_1, u and v are all real. Also note that the expression (3.17) contains only the symmetric terms of $|\phi_2|^2$ as the nonsymmetric terms integrate to zero in (3.16). Substituting the basis functions (3.10) and (3.12) into (3.16) gives the integral g_1 as

$$\begin{aligned} g_1 \;=\; & \left(\frac{r_{11} C}{2} + \frac{3 r_{13} C^3}{8}\right) (a_1 u^{-1} \sinh(2u) + b_1 v^{-1} \sin(2v)) \\ & + b \left(\frac{4r_{10} + 3r_{12} C^2}{4}\right) \left(\frac{\sin(\lambda_1 - 2v)}{\lambda_1 - 2v} + \frac{\sin(\lambda_1 + 2v)}{\lambda_1 + 2v}\right) \end{aligned}$$

$$+a_1\left(\frac{4r_{10}+3r_{12}C^2}{4\lambda_1^2+16u^2}\right)(4u\cos(\lambda_1)\sinh(2u)+2\lambda_1\sin(\lambda_1)\cosh(2u))$$

$$+a_1\frac{(r_{11}C+r_{13}C^3)}{2\lambda_1^2+2u^2}(u\sinh(2u)\cos(2\lambda_1)+\lambda_1\sin(2\lambda_1)\cosh(2u))$$

$$+b_1\frac{(r_{11}C+r_{13}C^3)}{2}\left(\frac{\sin(2\lambda_1-2v)}{2\lambda_1-2v}+\frac{\sin(2\lambda_1+2v)}{2\lambda_1+2v}\right)$$

$$+b_1\frac{r_{12}C^2}{4}\left(\frac{\sin(3\lambda_1-2v)}{3\lambda_1-2v}+\frac{\sin(3\lambda_1+2v)}{3\lambda_1+2v}\right)$$

$$+a_1\frac{r_{12}C^2}{18\lambda_1^2+8u^2}(2u\sinh(2u)\cos(3\lambda_1)+3\lambda_1\sin(3\lambda_1)\cosh(2u))$$

$$+a_1\frac{r_{13}C^3}{32\lambda_1^2+8u^2}(u\sinh(2u)\cos(4\lambda_1)+2\lambda_1\sin(4\lambda_1)\cosh(2u))$$

$$+b_1\frac{r_{13}C^3}{8}\left(\frac{\sin(4\lambda_1-2v)}{4\lambda_1-2v}+\frac{\sin(4\lambda_1+2v)}{4\lambda_1+2v}\right), \tag{3.18}$$

and the integral g_2 as

$$\begin{aligned} g_2 \;=\; & r_{20}+\frac{3r_{22}C^2}{4}+(6r_{21}C+5r_{23}C^3)\frac{\sin(\lambda_1)}{4\lambda_1} \\ & +(r_{20}+r_{22}C^2)\frac{\sin(2\lambda_1)}{2\lambda_1}+(4r_{21}C+5r_{23}C^3)\frac{\sin(3\lambda_1)}{24\lambda_1} \\ & +r_{22}C^2\frac{\sin(4\lambda_1)}{16\lambda_1}+r_{23}C^3\frac{\sin(5\lambda_1)}{40\lambda_1}. \end{aligned} \tag{3.19}$$

If the maximum temperature C is given then the decay rate a can be found from (3.15) and the heat-loss parameter λ can be found from (3.11). In general, when radiative heat loss occurs, (3.11) must be solved numerically (for example, by Newton's method) for λ. When the decay rate has been determined the coefficients $A(a)$ and $B(a)$ in (3.12) and the parameters a_1, b_1, u and v from (3.17) can all be calculated. Lastly, the integrals g_1 and g_2 are calculated from (3.18) and (3.19) and hence the power β can be determined from (3.16).

3.3. Results and discussion

The expressions for a, g_1 and g_2 can be simplified in the small and large heat-loss limits. In the limit of small heat loss

$$\lambda \to B_i + S(C^3+4C^2+6C+4) \quad \text{as} \quad B_i, S \to 0. \tag{3.20}$$

In this limit the integrals a, g_1 and g_2 become

$$\begin{aligned} & a = ik_1(1+i\alpha f(C))^{1/2}, \\ & g_1 = R_1(C)(a_1u^{-1}\sinh(2u)+b_1v^{-1}\sin(2v)), \\ & g_2 = 2R_2(C). \end{aligned} \tag{3.21}$$

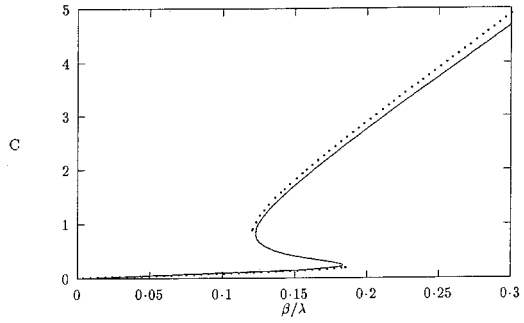

Figure 1. The steady-state temperature versus power curve (C versus β/λ) in the small Biot-number limit. The parameters are $B_i = 0{\cdot}1$, $S = 0$, $k = k_1 = 1$, $\alpha = 5 \times 10^{-3}$ and $\Delta x = 1 \times 10^{-3}$. Shown are the results by small Biot-number theory, (3.16) with a, g_1 and g_2 given by (3.21) (—), and the numerical solution $(\cdots)$.

The steady-state temperature versus power relationship in the small heat-loss limit, (3.16) with a, g_1 and g_2 given by (3.21), is the same as that found using the small Biot number theory of Kriegsmann [12]. Figure 1 shows the steady-state temperature versus power curve (C versus β/λ) in the limit of small Biot-number and no radiative heat loss. The parameters are $B_i = 0{\cdot}1, S = 0, k = k_1 = 1, \alpha = 5 \times 10^{-3}$ and $\Delta x = 1 \times 10^{-3}$. Shown are the results by small Biot number theory, (3.16) with a, g_1 and g_2 given by (3.21) (—), and the numerical solution $(\cdots)$. The comparison between the numerical and theoretical results is excellent, with only a small variation, of up to 6 percent at $\beta/\lambda = 0.3$, on the upper (hot) solution branch. No numerical results are available for the second branch (where $\mathrm{d}C/\mathrm{d}\beta < 0$) as this region of the solution is unstable. As the heat loss is small the temperature profile is nearly uniform. The approximate analytical solution is exact in this limit. As $\lambda \to 0$ the temperature profile becomes uniform, $T = \cos(\lambda^{1/2}x) \to C$, and the decay rate (3.21) is exact because of the uniform temperature.

In the limit of large heat-loss,

$$\lambda = \frac{\pi^2}{4} \quad \text{as} \quad B_i, S \to \infty. \tag{3.22}$$

In this limit the decay rate a is

$$a = ik_1 \left(1 + i\alpha \frac{J_1}{J_2}\right)^{1/2},$$

where

$$J_i = 2r_{i0} + \frac{4r_{i1}C}{\pi} + r_{i2}C^2 + \frac{8r_{i3}C^3}{3\pi}, \quad i = 1, 2, \tag{3.23}$$

while the integrals g_1 and g_2 become

$$g_1 = \left(\frac{r_{11}C}{2} + \frac{3r_{13}C^3}{8}\right)(a_1 u^{-1}\sinh(2u) + b_1 v^{-1}\sin(2v))$$

$$+(4r_{10} + 3r_{12}C^2)\left(\frac{\pi a_1}{\pi^2 + 16u^2}\cosh(2u) + \frac{\pi b_1}{\pi^2 - 16v^2}\cos(2v)\right)$$

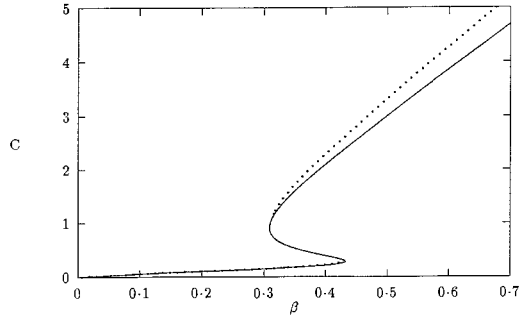

Figure 2. The steady-state temperature versus power curve (C versus β) in the large heat-loss limit. The parameters are $k = k_1 = 1, \alpha = 5 \times 10^{-3}$ and $\Delta x = 1 \times 10^{-3}$. Shown are the results by large heat-loss theory, (3.16) with a, g_1 and g_2 given by (3.23) and (3.24) (—), and the numerical solution $(\cdots)$.

$$-(r_{11}C + r_{13}C^3)\left(\frac{a_1}{\pi^2 + 4u^2}2u\sinh(2u) - \frac{b_1}{\pi^2 - 4v^2}2v\sin(2v)\right)$$

$$+\frac{r_{13}C^3}{8}\left(\frac{a_1}{\pi^2 + u^2}u\sinh(2u) - \frac{b_1 v}{\pi^2 - v^2}\sin(2v)\right), \tag{3.24}$$

$$g_2 = r_{20} + \frac{8r_{21}C}{3\pi} + \frac{3r_{22}C^2}{4} + \frac{32r_{23}C^3}{15\pi}.$$

Figure 2 shows that steady-state temperature versus power curve (C versus β) in the large heat-loss limit ($B_i, S \to \infty$). The parameters are $k = k_1 = 1, \alpha = 5 \times 10^{-3}$ and $\Delta x = 1 \times 10^{-3}$. Shown are the results by large heat-loss theory, (3.16) with a, g_1 and g_2 given by (3.23) and (3.24) (—), and the numerical solution $(\cdots)$. On the lower (cool) branch the theory and the numerical solution are the same to graphical accuracy with the critical β at which the solution jumps to the upper (hot) branch, and hence undergoes thermal runaway, accurately predicted by the theory. On the upper (hot) branch the comparison is still good with a variation, of up to 9 percent at $\beta = 0{\cdot}7$. This discrepancy is due to the form of the basis functions being less realistic at high temperature levels. For example, the basis function for the electric-field amplitude assumes uniform temperature in the slab, which is less valid as the temperature increases. Moreover, the assumed symmetry of the temperature profile breaks down. The increased electrical conductivity causes decay of the electric-field amplitude in the slab. As the amplitude of the microwave radiation which penetrates into the centre of the slab is reduced, there is less heat absorption and consequently a non-symmetric temperature profile occurs.

Figure 3 and 4 show the temperature profile and the electric-field amplitude for the same parameters as Figure 2 with a power level $\beta = 0{\cdot}4$. Shown are the results by large heat-loss theory, (3.10) and (3.12) with a, g_1 and g_2 given by (3.23) and (3.24) (—), and the numerical solution $(\cdots)$. This power level corresponds to the lower (cool) solution branch just before thermal runaway occurs. As the decay of the electric-field amplitude is small (around 0.5 percent) heat is absorbed fairly evenly across the slab resulting in a symmetric temperature profile. Consequently the comparison between the theoretical and numerical temperature profiles is excellent with the maximum temperature varying by no more than 3 percent. Also, the temperature is fairly uniform in the slab (as $C \approx 0{\cdot}2$ is small) so the electric-field amplitude, as predicted by the approximate theory, is very close to the numerical solution.

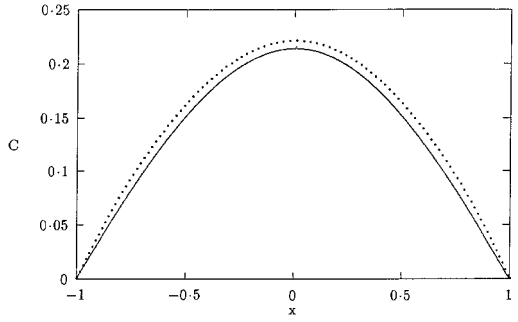

Figure 3. The steady-state temperature profile versus x in the large heat-loss limit. The parameters are $k = k_1 = 1, \beta = 0{\cdot}4, \alpha = 5 \times 10^{-3}$ and $\Delta x = 1 \times 10^{-3}$. Shown are the data by large heat-loss theory, (3.10) with a, g_1 and g_2 given by (3.23) and (3.24) (—), and the numerical solution $(\cdots)$.

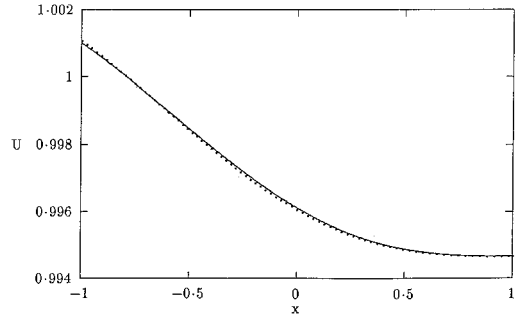

Figure 4. The steady-state electric-field amplitude versus x in the large heat-loss limit. The parameters are $k = k_1 = 1, \beta = 0{\cdot}4, \alpha = 5 \times 10^{-3}$ and $\Delta x = 1 \times 10^{-3}$. Shown are the data by large heat-loss theory, (3.12) with a, g_1 and g_2 given by (3.23) and (3.24) (—), and the numerical solution $(\cdots)$.

Figure 5 shows the steady-state temperature versus power curve (C versus β/B_i) for small Biot and radiation numbers. The parameters are $B_i = 0.1, S = 0.1, k = k_1 = 1, \alpha = 5 \times 10^{-3}$ and $\Delta x = 1 \times 10^{-3}$. Shown are the data by the theory, (3.16) with a, g_1 and g_2 given by (3.15), (3.18) and (3.19) (—), and the numerical solution $(\cdots)$. In this case only the lower (cool) solution branch can be described using the small heat-loss theory (3.21). This occurs because the radiative heat-loss increases nonlinearly as the power, and hence the temperature

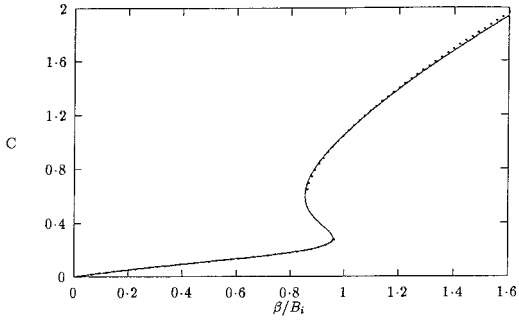

Figure 5. The steady-state temperature versus power curve (C versus β/B_i) for small Biot and radiation numbers. The parameters are $B_i = 0{\cdot}1, S = 0{\cdot}1, k = k_1 = 1, \alpha = 5 \times 10^{-3}$ and $\Delta x = 1 \times 10^{-3}$. Shown are the data by the theory, (3.16) with a, g_1 and g_2 given by (3.15), (3.18) and (3.19) (—), and the numerical solution $(\cdots)$.

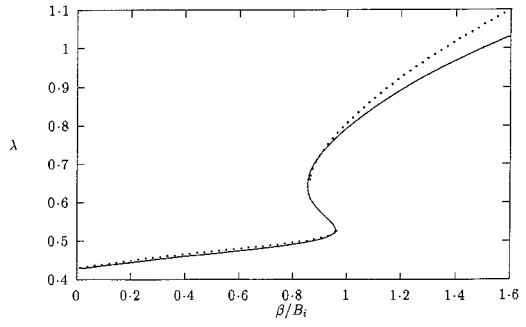

Figure 6. The heat-loss parameter versus power (λ versus β/B_i) for small Biot and radiation numbers. The parameters are $B_i = 0{\cdot}1, S = 0{\cdot}1, k = k_1 = 1, \alpha = 5 \times 10^{-3}$ and $\Delta x = 1 \times 10^{-3}$. Shown are the data by the theory, (3.16) with a, g_1 and g_2 given by (3.15), (3.18) and (3.19) (—), and the numerical solution $(\cdots)$.

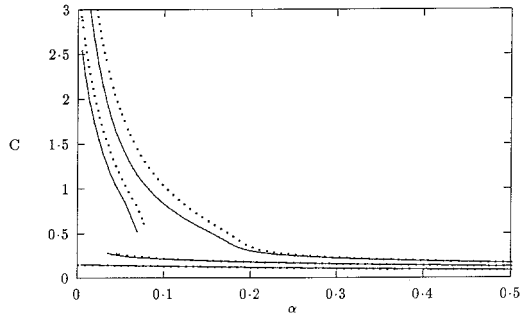

Figure 7. The steady-state temperature versus decay rate (C versus α) for the large heat-loss limit. The parameters are $k = k_1 = 1, \Delta x = 1 \times 10^{-3}$ for $\beta = 0{\cdot}15, 0{\cdot}3$ and $0{\cdot}6$. Shown are the data by theory, (3.16) with a, g_1 and g_2 given by (3.23) and (3.24) (—), and the numerical solution $(\cdots)$.

C, increases. The analytical and the numerical solutions differ by no more than 1 percent (at $\beta/B_i = 1{\cdot}6$) on both solution branches. Figure 6 shows the heat-loss parameter versus power (λ versus β/B_i) for the same parameters as Figure 5. Shown are the data by the theory, (3.11) with a, g_1 and g_2 given by (3.15), (3.18) and (3.19) (—), and the numerical solution $(\cdots)$. As the Biot and radiation numbers are small the lower (cool) solution branch corresponds to the small heat-loss case, with λ given approximately by (3.20). However as the temperature C increases the radiative heat-loss also increases and the expression (3.11) must be used to calculate λ. As the power (and the temperature C) increase further the large heat-loss limit, $\lambda \to \pi^2/4$, is approached on the upper (hot) solution branch, where the analytical and numerical solutions vary, by up to 9 percent at $\beta/B_i = 1{\cdot}6$.

3.4. VALIDITY OF THE APPROXIMATE SOLUTIONS

The basis functions for the temperature and the electric-field amplitude are valid in the limit of low thermal absorptivity and uniform temperature respectively. These assumptions are true in the small heat-loss limit as the temperature profile is nearly uniform, and the thermal absorptivity is small (small heat-loss implies small thermal absorptivity at the steady-state). Consequently, the approximate analytical solutions are very accurate in this case (see Figure 1).

Figure 7 shows the steady-state temperature versus decay rate (C versus α) for the large heat-loss limit. The parameters are $k = k_1 = 1, \Delta x = 1 \times 10^{-3}$ for $\beta = 0{\cdot}15, 0{\cdot}3$ and $0{\cdot}6$.

Shown are the data by theory, (3.16) with a, g_1 and g_2 given by (3.23) and (3.24) (—), and the numerical solution $(\cdots)$. For a given value of the decay rate α the temperature increases as the power β increases. Hence $\beta = 0{\cdot}15$ is the lowest curve and $\beta = 0{\cdot}6$ is the highest curve on the graph. As the decay rate α increases lower slab temperatures are obtained. This is because the electric-field amplitude decays more quickly in the material limiting the total energy which can be absorbed. For the lowest power level $(\beta = 0{\cdot}15)$ the temperature is very small for all values of α as it remains on the lower (cool) branch of the S-shaped power versus temperature curve. For the larger values of the power β however, the solution is on the upper branch for small α and on the lower branch for large α.

The comparison between the theoretical and numerical results is excellent at lower temperature levels, which generally corresponds to the lower branch of the S-shaped curve. When the decay rate α is large the approximate theory remains accurate because the temperature C is small. As the slab's temperature is nearly uniform in this limit the theoretical electrical-field amplitude (3.13) is very close to the exact numerical value. The large decay of the electric-field amplitude results in a non-symmetric temperature profile though. However, because C is small the approximate analytical solution predicts a temperature maximum which is very accurate even though the analysis assumes a symmetric temperature profile.

For smaller values of α and larger values of β the solution lies on the upper (hot) branch of the S-shaped curve. Even though the assumptions underlying the approximate solution have broken down in this regime, the approximate analytical solutions are still reasonably close to the numerical results.

4. Conclusion

An approximate analytical model has been developed to describe the steady-state microwave heating of a one-dimensional slab subject to both convective and radiative heat loss. The approximate model incorporates the Arrhenius law as the temperature dependency for the electrical conductivity and the thermal absorptivity. The approximate solutions for the steady-state electric-field amplitude and the temperature are in excellent agreement with the full numerical solutions over a range of examples. In particular, the approximate temperature versus power relationship gives excellent predictions on the lower branch of the S-shaped curve, including the critical power level at which thermal runaway occurs. On the upper branch of the S-shaped curve the theoretical predictions show some variation from the numerical solutions but are still quite close. The approximate solutions require about two orders of magnitude less computational effort than does the steady-state numerical solutions hence the approximate model allows an accurate prediction of thermal runaway to be obtained at a much smaller computational cost.

The one-dimensional model, although idealised, lays the ground work for the development in the future of approximate solutions for more physically realistic two and three dimensional slabs and blocks. These higher-order analytical solutions can be obtained by extending the Galerkin technique used here. The resulting approximate solutions however, will be longer and more complicated than those obtained here in the one-dimensional case. The two and three dimensional approximate solutions will allow the accurate prediction of thermal runaway in real industrial heating problems for which the full numerical solution would be computationally prohibitive. This is particularly valuable if real time control over the industrial microwave heating application is required.

Acknowledgement

The authors wish to thank the anonymous referees for some useful comments.

A. Appendix: The numerical scheme

The accuracy of the approximate analytical solutions obtained in Section 3 are examined by comparison with numerical solutions of the steady-state version of the governing Equations (2.9) with boundary conditions (2.11). The steady-state solution is

$$\mathbf{T} = [t_i], \quad \mathbf{U} = [u_i], \quad i = 1, \ldots, n,$$

where

$$\begin{aligned} t_i &= T(-1 + (i-1)\Delta x), \\ u_i &= U(-1 + (i-1)\Delta x), \\ n &= 1 + \frac{2}{\Delta x} \end{aligned} \tag{A.1}$$

and Δx is the spatial grid size. A centred finite-difference scheme is used for the spatial discretisation of the governing Equations (2.9) and boundary conditions (2.11). This results in the discretised equations having the matrix form

$$A\mathbf{T} = \mathbf{b}, \quad B\mathbf{U} = \mathbf{d}, \tag{A.2}$$

where the matrices A and B have elements

$$\begin{aligned} &a_{i,i} = 1, \quad a_{i,i-1} = a_{i,i+1} = -\tfrac{1}{2}, \quad i = 2, \ldots, n-1, \\ &b_{i,i} = 1 - (\Delta x)^2 k_1^2 (1 + i\alpha f(t_i)), \\ &b_{i,i-1} = b_{i,i+1} = -\tfrac{1}{2}, \quad i = 2, \ldots, n-1, \\ &a_{1,1} = 1 + \Delta x B_i + \Delta x S(t_1^3 + 4t_1^2 + 6t_1 + 4), \\ &a_{n,n} = 1 + \Delta x B_i + \Delta x S(t_n^3 + 4t_n^2 + 6t_n + 4), \\ &a_{1,2} = a_{n,n-1} = -1, \\ &b_{1,1} = 1 - \frac{\Delta x k i}{2} + \frac{(\Delta x)^2 k_1^2}{2}(1 + i\alpha f(t_1)), \\ &b_{n,n} = 1 - \frac{\Delta x k i}{2} + \frac{(\Delta x)^2 k_1^2}{2}(1 + i\alpha f(t_n)), \\ &b_{1,2} = b_{n,n-1} = -1, \end{aligned} \tag{A.3}$$

with all other elements equal to zero. The vectors **b** and **d** have elements

$$\begin{aligned} &b_i = (\Delta x)^2 \beta f(t_i)|u_i|^2, \quad i = 1, \ldots, n, \\ &d_1 = 2ik\Delta x, \quad d_i = 0, \quad i = 2, \ldots, n. \end{aligned} \tag{A.4}$$

The system of coupled nonlinear Equations (A.2)–(A.4) is solved via the iteration scheme

$$A^{(p)}\mathbf{T}^{(p+1)} = \mathbf{b}^{(p)}, \quad B^{(p)}\mathbf{U}^{(p+1)} = \mathbf{d}^{(p)}, \quad p = 1, 2, \ldots, \tag{A.5}$$

where the initial matrices and vectors, $A^{(0)}, B^{(0)}, \mathbf{b}^{(0)}$ and $\mathbf{d}^{(0)}$, are evaluated at the ambient temperature of zero. The iteration scheme (A.5) is assumed to have converged when the difference in the temperature at the centre of the slab over two iterations is less than a small tolerance ε.

$$\left| t_{\frac{n}{2}}^{(p+1)} - t_{\frac{n}{2}}^{(p)} \right| < \varepsilon. \tag{A.6}$$

The scheme (A.5) normally takes between 10 and 20 iterations to converge using (A.6) with $\varepsilon = 1 \times 10^{-5}$.

References

1. A. C. Araneta, M. E. Brodwin and G. A. Kriegsmann, High temperature microwave characterisation of dielectric rods. *IEEE, MIT* 32 (1984) 1328–1336.
2. J. M. Hill and T. R. Marchant, Modelling microwave heating. *Appl. Math. Modelling* 20 (1996) 3–15.
3. N. F. Smyth, Microwave heating of bodies with temperature dependent properties. *Wave Motion* 12 (1990) 171–186.
4. T. R. Marchant and A. H. Pincombe, Microwave heating of materials with temperature dependent wavespeed. *Wave Motion* 19 (1994) 67–81.
5. A. H. Pincombe and N. F. Smyth, Microwave heating of materials with low conductivity. *Proc. Roy. Soc. Lond. A* 433 (1991) 479–498.
6. G. Roussy, A. Bennani and J. Thiebaut. Temperature runaway of microwave irradiated materials. *J. Appl. Phys.* 62 (1987) 1167–1170.
7. J. M. Hill and N. F. Smyth, On the mathematical analysis of hotspots arising from microwave heating. *Math. Eng. in Industry* 2 (1990) 267–278.
8. T. R. Marchant, Microwave heating of materials with impurities. *J. Engng. Math.* 28 (1994) 379–400.
9. S. P. Zhu, Y. L. Zhang and T. R. Marchant, A DRBEM model for microwave heating. *Appl. Math. Modelling* 19 (1995) 287–297.
10. G. A. Kriegsmann, M. E. Brodwin and D. G. Watters, Microwave heating of a ceramic halfspace. *SIAM J. Appl. Math.* 50 (1990) 1088–1098.
11. G. A. Kriegsmann, Microwave heating of ceramics, In B. Sleeman and R. Jarvis, (eds.), *Ordinary and Partial Differential Equations 3* Longman House (1991) 45–56.
12. G. A. Kriegsmann, Thermal runaway in microwave heated ceramics: a one-dimensional model. *J Appl. Phys.* 71 (1992) 1960–1966.
13. T. R. Marchant and G. A. Kriegsmann, Thermal runaway of microwave heated materials with small losses. Research report 96/11 Uni. of Wollongong, Aust. (1996) 22 pp.
14. A. M. Portis, *Electromagnetic fields:sources and media*. John Wiley and Sons New York (1978) 775 pp.
15. T. R. Marchant, Thermal runaway during microwave welding. *Conf. Proc. AEMC* (1996) 201–208.
16. J. M. Hill and M. J. Jennings, Formulation of model equations for heating by microwave radiation. *Appl. Math. Modelling* 17 (1993) 369–379.